Published OnlineFirst September 24, 2014; DOI: 10.1158/0008-5472.CAN-14-1916

Cancer Research

Plk1 Inhibition Enhances the Efficacy of Androgen Signaling Blockade in Castration-Resistant Prostate Cancer

Zhe Zhang, Xianzeng Hou, Chen Shao, et al.

Cancer Res 2014;74:6635-6647. Published OnlineFirst September 24, 2014.

Published OnlineFirst September 24, 2014; DOI: 10.1158/0008-5472.CAN-14-1916

Therapeutics, Targets, and Chemical Biology

Cancer Research

Plk1 Inhibition Enhances the Efficacy of Androgen Signaling Blockade in Castration-Resistant Prostate Cancer

Zhe Zhang[1,2], Xianzeng Hou[1,3], Chen Shao[1], Junjie Li[4], Ji-Xin Cheng[4], Shihuan Kuang[5], Nihal Ahmad[6], Timothy Ratliff[7], and Xiaoqi Liu[1,7]

Abstract

Prostate cancer is thought to be driven by oxidative stress, lipid metabolism, androgen receptor (AR) signaling, and activation of the PI3K–AKT–mTOR pathway, but it is uncertain how they may become coordinated during progression to castration-resistant disease that remains incurable. The mitotic kinase polo-like kinase 1 (Plk1) is elevated in prostate cancer, where its expression is linked to tumor grade. Notably, Plk1 signaling and lipid metabolism were identified recently as two of the top five most upregulated pathways in a mouse xenograft model of human prostate cancer. Herein, we show that oxidative stress activates both the PI3K–AKT–mTOR pathway and AR signaling in a Plk1-dependent manner in prostate cells. Inhibition of the PI3K–AKT–mTOR pathway prevented oxidative stress-induced activation of AR signaling. Plk1 modulation also affected cholesteryl ester accumulation in prostate cancer via the SREBP pathway. Finally, Plk1 inhibition enhanced cellular responses to androgen signaling inhibitors (ASI) and overcame ASI resistance in both cultured prostate cancer cells and patient-derived tumor xenografts. Given that activation of AR signaling and the PI3K–AKT–mTOR pathway is sufficient to elevate SREBP-dependent expression of key lipid biosynthesis enzymes in castration-resistant prostate cancer (CRPC), our findings argued that Plk1 activation was responsible for coordinating and driving these processes to promote and sustain the development of this advanced stage of disease. Overall, our results offer a strong mechanistic rationale to evaluate Plk1 inhibitors in combination drug trials to enhance the efficacy of ASIs in CRPC. *Cancer Res; 74(22); 6635–47. ©2014 AACR.*

Introduction

Prostate cancer is the second leading cause of death due to cancer in males in the United States, with 233,000 news cases and 29,480 deaths estimated in 2014 (1). Treatment options for late-stage disease are limited. Androgen-deprivation therapy is initially effective, but remissions are temporary and the disease eventually progresses to castration-resistant prostate cancer (CRPC). Evidence from experimental and clinical studies suggests that prostate cancer cells are exposed to increased oxidative stress. A potential role for reactive oxygen species (ROS) in the regulation of cellular processes controlling malignant transformation holds a lot of promise in understanding prostate cancer, as this will open doors for the development of novel therapeutics for the disease (2). Besides acting as a DNA-damaging agent, moderately elevated levels of ROS may act as secondary messengers that contribute to the oncogenic phenotype by activating many transcription factors and signaling pathways. Therefore, identification of prostate-specific signaling pathways in response to oxidative stress will provide novel targets for treatment options (2).

The androgen receptor (AR) is a critical effector of prostate cancer development and progression. In response to androgen, activated AR is translocated from the cytoplasm into the nucleus, acting as a transcription factor that activates many downstream proteins, such as prostate-specific antigen (PSA). Enough evidence suggests that AR signaling continues to be essential for prostate cancer development even after castration. In support, current approaches to treat CRPC are to delay or replace treatment with cytotoxic agents, such as docetaxel, with androgen signaling inhibitors (ASI), such as abiraterone and enzalutamide (previously MDV3100; refs. 3, 4). However, overall survival was only improved by 5 or 2 months in the recent phase III trials that compared abiraterone or enzalutamide with placebo in patients with CRPC (4–6). Therefore, new mechanism-based studies are urgently needed to identify targets and strategies to overcome ASI resistance, thus achieving effective management of CRPC.

It has been established that the PI3K–AKT–mTOR pathway plays a critical role in prostate cancer cell survival. The PI3Ks are enzymes that are responsible for generation of the second messenger phosphatidylinositol 3,4,5-triphosphate (PIP3) that

[1]Department of Biochemistry, Purdue University, West Lafayette, Indiana. [2]State Key Laboratory for Agrobiotechnology and Department of Microbiology, China Agricultural University, Beijing, China. [3]Department of Neurosurgery, Qianfoshan Hospital affiliated to Shandong University, Jinan, China. [4]Department of Biomedical Engineering, Purdue University, West Lafayette, Indiana. [5]Department of Animal Sciences, Purdue University, West Lafayette, Indiana. [6]Department of Dermatology, University of Wisconsin, Madison, Wisconsin. [7]Purdue Center for Cancer Research, Purdue University, West Lafayette, Indiana.

Z. Zhang and X. Hou contributed equally to this article.

Corresponding Author: Xiaoqi Liu, Department of Biochemistry, Purdue University, 175 S. University Street, West Lafayette, IN 47907. Phone: 765-496-3764; Fax: 765-494-7897; E-mail: liu8@purdue.edu

doi: 10.1158/0008-5472.CAN-14-1916

Published OnlineFirst September 24, 2014; DOI: 10.1158/0008-5472.CAN-14-1916

activates AKT, which mediates activation of the mTOR complex, a kinase that controls protein translation via activation of S6K and S6. The tumor-suppressor PTEN (phosphatase and tensin homolog) acts as a major antagonist to the PI3K pathway. Although prostate-specific knockout of PTEN leads to invasive prostate cancer and ultimately to metastatic cancer in mice (7), loss-of-function PTEN mutations are detected in less than 5% of primary prostate tumors, suggesting that additional mechanisms might be responsible for activation of the PI3K–AKT–mTOR pathway in prostate cancer.

Increasing evidence in recent years suggests that deregulation of lipid metabolism is another hallmark of prostate cancer. For example, high contents of both free cholesterol and cholesteryl esters (CE) of prostate tissues correlate with the presence of malignancy, likely due to abnormalities in lipid homeostasis (8). Key players in the regulation of lipid metabolism are the sterol regulatory element binding proteins (SREBP), a family of three transcription factors (SREBP-1a, SREBP-1c, SREBP-2) that are attached to the endoplasmic reticulum as inactive forms. When sterol levels are low, SREBPs will be activated by SREBP-cleavage-activating protein (SCAP) to drive expression of enzymes needed for lipid synthesis, such as fatty acid synthase (FAS), HMGCoA-R, and low-density lipoprotein receptor (LDL-R; 9). Of note, both the PI3K–AKT–mTOR and AR pathways act upstream of the SREBP pathway, resulting in elevation of lipid synthesis (Fig. 7; refs. 10, 11). Cholesterol can serve as a precursor to drive *de novo* steroidogenesis to increase intratumoral androgen levels, thus activating AR signaling (12). Cholesterol, combined with increased levels of fatty acid, will also increase the formation of lipid rafts, which have documented roles in activation of the PI3K–AKT–mTOR pathway and cell migration (Fig. 7). Despite all these progresses, whether and how oxidative stress and various signaling pathways are coordinated to contribute to CRPC is not known.

Polo-like kinase 1 (Plk1) is a regulator of many cell-cycle events, such as mitotic entry and cytokinesis (13). A close correlation between the level of Plk1 expression and prognosis has been documented. Therefore, it has been proposed that inhibition of Plk1 is an important strategy for enhancement of cancer therapy (13). Indeed, the Plk1 inhibitor BI2536 is in phase II clinical studies for patients with various cancers. Significantly, Plk1 is overexpressed in prostate cancer and is linked to higher grade tumors, suggesting that Plk1 is involved in tumorigenesis and progression in this tumor entity (14). Furthermore, RNAi-mediated Plk1 knockdown causes induction of mitotic catastrophe in prostate cancer cells, suggesting that Plk1 might be a target for prostate cancer management (14). Of note, Plk1 and lipid metabolism are two of the top five most-upregulated pathways after castration in a microarray analysis of a prostate cancer xenograft model (15). However, the molecular mechanisms responsible for these encouraging observations are still undefined. Our data explain how castration-associated Plk1 elevation induces activation of the PI3K–AKT–mTOR and AR pathways and increase of lipid biosynthesis, eventually resulting in CRPC. Our finding supports the notion that inhibition of Plk1 is a novel avenue to enhance the efficacy of ASI in CRPC.

Materials and Methods

Cell culture

RWPE-1 cells were cultured in keratinocyte serum-free medium (K-SFM; Invitrogen; 17005-042) supplemented with 50 μg/mL bovine pituitary extract (BPE), 5 ng/mL epidermal growth factor (EGF; Human Recombinant), 100 U/mL penicillin, and 100 U/mL streptomycin at 37°C in 8% CO_2. HEK293T and DU145 cells were cultured in Dulbecco's Modified Eagle Medium (DMEM) supplemented with 10% (*v*/*v*) fetal bovine serum (FBS), 100 U/mL penicillin, and 100 U/mL streptomycin at 37°C in 8% CO_2. PC3 cells were cultured in F12K supplemented with 10% (*v*/*v*) FBS, 100 U/mL penicillin, and 100 U/mL streptomycin at 37°C in 8% CO_2. LNCaP, C4-2, 22Rv1, and MR49F cells were cultured in RPMI-1640 (ATCC) supplemented with 10% FBS (*v*/*v*), 100 U/mL penicillin, and 100 U/mL streptomycin at 37°C in 8% CO_2. For MR49F cells, 10 μmol/L MDV3100 was added to the medium to maintain the MDV3100 resistance.

RNAi

siRNAs targeting AR splice variants (AR-vs) in 22Rv-1 cells were synthesized by Thermo Scientific Dharmacon. The targeting sequences are AAUCUUGAGGGUGUUUGGAGUUU for AR-V1 and AAUGACCAGACCCUGAAGAAAUU for AR-V7. Control siRNA was ordered from Santa Cruz Biotechnology (sc-37007). Lipofectamine 2000 Reagent (Invitrogen, 11668-019) was used for DNA or siRNA transfection.

Drugs

Pyrrolidine dithiocarbamate, diamide, dihydrotestosterone, R1881, insulin, LY294002, and nocodazole were purchased from Sigma. Diphenyleneiodonium chloride and BI2536 were purchased from Calbiochem and Symansis, respectively. Abiraterone, MDV3100 (enzalutamide), MK2206, and rapamycin were purchased from Selleckchem.

Western blotting

Harvested cells were lysed in TBSN buffer (20 mmol/L Tris, pH 8.0, 150 mmol/L NaCl, 1.5 mmol/L EDTA, 5 mmol/L EGTA, 0.5% Nonidet P-40, and 0.5 mmol/L Na_3VO_4) supplemented with proteinase inhibitors. The lysates were resolved by SDS-PAGE and transferred to Whatman Westran polyvinylidenedifluoride (PVDF) membrane (Sigma; Z671088), followed by incubation with antibodies against Plk1 (Santa Cruz Biotechnology; sc-17783), phospho-AKT-S473 (Cell Signaling Technology; 9271), phospho-AKT-T308 (Cell Signaling Technology; 13038), AKT (Cell Signaling Technology; 9272), phospho-S6K (Cell Signaling Technology; 9205), phospho-S6 (Cell Signaling Technology; 2211), S6 (Cell Signaling Technology; 2217), phospho-NFκB (Cell Signaling Technology; 3033), NFκB (Santa Cruz Biotechnology; sc-372), AR (Santa Cruz Biotechnology; sc-7305), γ-tubulin (Sigma; T3559), p84 (Abcam; ab487), Twist1 (Sigma; SAB1411370), SREBP1 (Santa Cruz Biotechnology; sc-367), SREBP2 (Santa Cruz Biotechnology; sc-5603), phospho-GSK3β (Cell Signaling Technology; 9322), GSK3β (BD Biosciences; 610201), FAS (BD Biosciences; 610962), HMG-CoA reductase (EMD Millipore; ABS229), cleaved-PARP (EMD Millipore; AB3620), PSA (Cell Signaling Technology; 5365), and β-actin (Sigma; A5441).

Published OnlineFirst September 24, 2014; DOI: 10.1158/0008-5472.CAN-14-1916

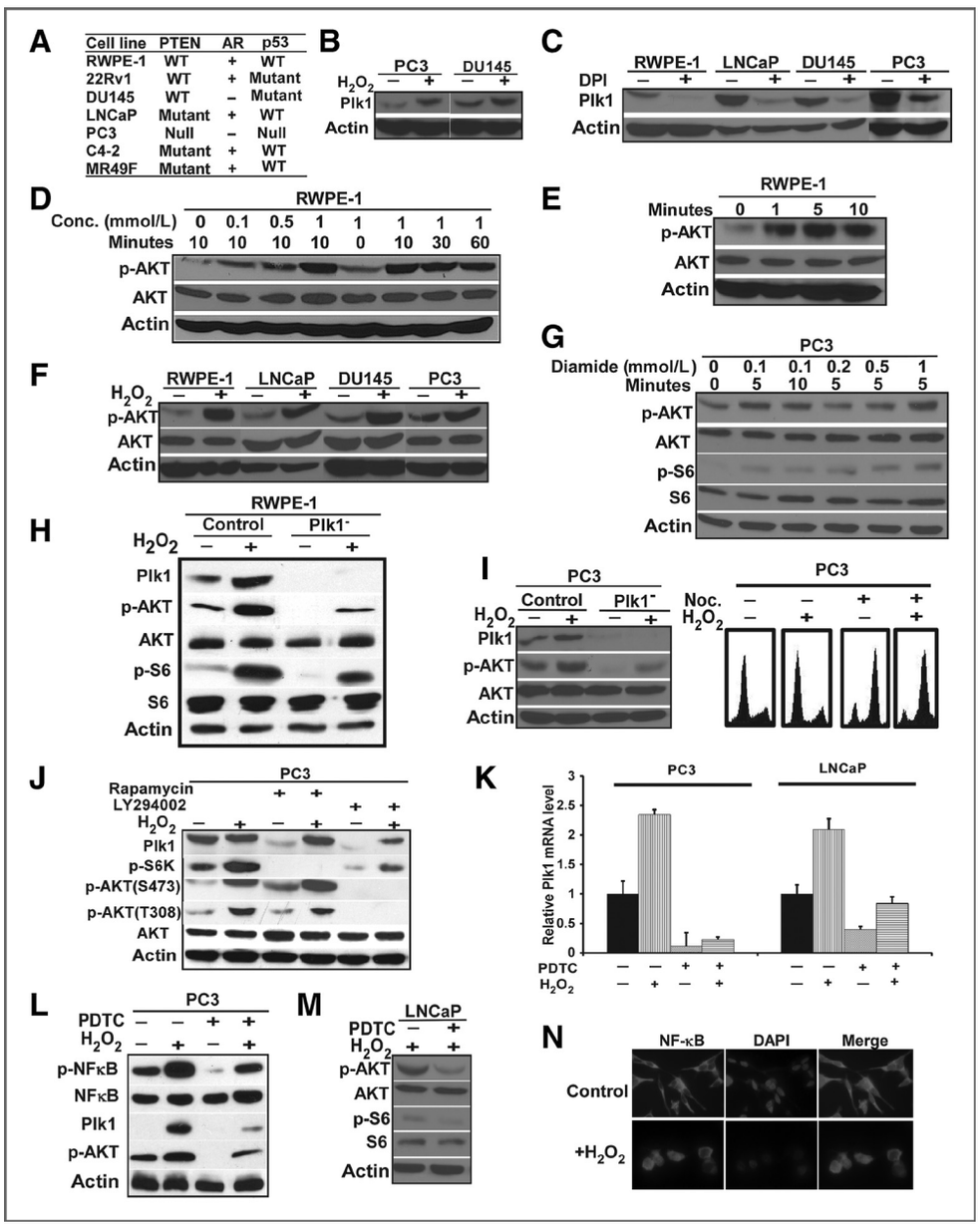

Figure 1. Oxidative stress activates the PI3K–AKT–mTOR pathway in a Plk1-dependent manner in prostate cells. A, genetic backgrounds of prostate cells used in the study. B, moderate oxidative stress leads to increased levels of Plk1 in prostate cancer cells. PC3 and DU145 cells were treated with or without 1 mmol/L of H_2O_2 for 5 minutes and harvested for anti-Plk1 immunoblotting. C, inhibition of oxidative stress leads to reduced levels of Plk1 protein. RWPE-1, LNCaP, DU145, and PC3 cells were treated with or without 20 μmol/L of diphenyleneiodonium chloride (DPI), an inhibitor of NADPH oxidase, in the presence of 200 ng/mL of nocodazole for 10 hours and harvested. D and E, oxidative stress activates the PI3K–AKT–mTOR pathway in RWPE-1 cells. RWPE-1 cells were treated with different concentrations of H_2O_2 for 10 minutes (the left four lanes in D) or with 1 mmol/L of H_2O_2 for different times (the right four lanes in D and E) as indicated and harvested for anti-p-AKT immunoblotting. F, oxidative stress activates the PI3K–AKT–mTOR pathway in multiple prostate cell lines. RWPE-1, LNCaP, DU145, and PC3 cells were treated with 1 mmol/L of H_2O_2 for 5 minutes and harvested. G, PC3 cells were treated with diamide for various conditions as indicated. H and I, oxidative stress–induced activation of the PI3K–AKT–mTOR pathway is Plk1 dependent. RWPE-1 (H) or PC3 (I) cells were depleted of Plk1 by infection with lentivirus. After selection for infection-positive cells with puromycin for 36 hours, cells were treated with 1 mmol/L of H_2O_2 for 5 minutes and harvested for immunoblotting or FACS. I, right, cells were treated with or without nocodazoel (Noc.) for 12 hours before treatment with H_2O_2. J, inhibition of the PI3K–AKT–mTOR pathway did not affect oxidative stress–induced elevation of Plk1 protein. PC3 cells were preincubated with two inhibitors of the PI3K–AKT–mTOR pathways (25 μmol/L of LY294002 for 1 hour or 100 nmol/L of rapamycin for 2 hours), treated with 1 mmol/L H_2O_2 for 5 minutes, and harvested for immunoblotting. K and L, oxidative stress–induced elevation of Plk1 is NF-κB dependent. PC3 or LNCaP cells were incubated with 100 μmol/L of pyrrolidine dithiocarbamate (PDTC) for 10 minutes, treated with or without 1 mmol/L of H_2O_2 for 5 minutes, and harvested for RT-PCR to measure Plk1 mRNA levels (K) or to immunoblot with antibodies indicated (L). M, oxidative stress–induced activation of the PI3K–AKT–mTOR pathway is NF-κB dependent. LNCaP cells were incubated with 100 μmol/L of PDTC for 30 minutes, treated with 1 mmol/L of H_2O_2 for 5 minutes and harvested for immunoblotting. N, oxidative stress increased nuclear accumulation of NF-κB. LNCaP cells were treated with 1 mmol/L of H_2O_2 for 5 minutes and harvested for immunofluorescent staining against NF-κB.

Published OnlineFirst September 24, 2014; DOI: 10.1158/0008-5472.CAN-14-1916

Cytoplasmic and nuclear protein extract preparations

Cytoplasmic and nuclear protein extracts were prepared with a kit from ActiveMotif (catalog no., 40410) according to the manufacturer's instructions.

Immunofluorescent staining

Cells were fixed with 4% paraformaldehyde for 10 minutes, washed with 0.1% Triton X-100 PBS, and permeabilized with methanol for 2 minutes. Upon wash with 0.1% Triton X-100 PBS, cells were blocked with 3% bovine serum albumin in PBS for 10 minutes, and incubated with anti-AR antibody for 2 hours at room temperature, followed by incubation with Alexa Fluor 555 goat anti-mouse IgG (H+L) secondary antibody (Invitrogen; A21424) and 4,6-diamidino-2-phenylindole (DAPI; Sigma) for 1 hour.

Depletion and overexpression of Plk1

HEK293T cells in 10-cm dishes were cotransfected with 4 μg of pHR'-CMV-ΔR 8.20vpr, 2 μg of pHR'-CMV-VSV-G, and 4 μg of pLKO.1-Plk1 for depletion of Plk1 or LV-CMV-Plk1 for overexpression of Plk1. Supernatants were collected every 12 hours after 24 hours of transfection. Viruses were filtered through a 0.45-μm pore size filter, concentrated by spin at 20,000 rpm for 2 hours, resuspended in TNE buffer (50 mmol/L Tris–HCl, pH 7.8, 130 mmol/L NaCl, 1 mmol/L EDTA), and rotated overnight at 4°C. Infections were carried out in the presence of 10 μg/mL of polybrene and 10 mmol/L of HEPES, followed by selection with 1 μg/mL of puromycin for at least 36 hours.

Cholesteryl ester measurement by Raman spectrometry

CE measurement by Raman spectrometry was performed with a compound Raman microscope as described previously (8).

Patient-derived xenograft model

Mice carrying LuCaP35CR tumors were obtained from Dr. Robert Vessella at University of Washington (Seattle, WA; ref. 16). Tumors were amplified by cutting the original tumors into about 20 to 30 mm^3 pieces and then implanted into precastrated nude mice. After amplifying enough tumors, tumors were harvested and cut into about 20 to 30 mm^3 pieces before implanting into 16 precastrated nude mice. When tumors reached 250 to 300 mm^3, mice were randomly separated into four groups (four mice in each group) for different treatments. Tumor volume was calculated as length × $width^2/2$. BI2536 was dissolved in 0.1 mol/L HCl and then diluted in 0.9% NaCl for injection. Blood was collected once a week and serum PSA level was measured using the PSA ELISA Kit (Abnova; KA0208).

Results

Plk1 acts upstream of the PI3K–AKT–mTOR pathway during oxidative stress

To understand how Plk1 is involved in CRPC, we treated prostate cells with oxidative stress, as castration induces oxidative stress *in vivo*, and treatment with hydrogen peroxide (H_2O_2) can partially mimic cellular events after castration. Genetic backgrounds of different prostate cell lines we used in this study are indicated in Fig. 1A. Treatment of two prostate cancer cell lines, PC3 and DU145, with H_2O_2 led to increased levels of Plk1 (Fig. 1B). In agreement, inhibition of oxidative stress with diphenyleneiodonium chloride reduced the levels of Plk1 in multiple prostate cell lines, including RWPE-1, a nontransformed prostate cell line that is established by transfection with a single copy of the human papilloma virus 18 into epithelial cells derived from the peripheral zone of a histologically normal adult human prostate (Fig. 1C). Considering that the PI3K–AKT–mTOR pathway has an established role in prostate cancer, we next asked whether oxidative stress results in activation of this pathway as well. As indicated in Fig. 1D–F, treatment of cells with H_2O_2 led to phosphorylation of AKT in multiple prostate cell lines, including RWPE-1. We also asked whether oxidative stress other than H_2O_2 can cause activation of the PI3K–AKT–mTOR pathway as well. Diamide oxidizes cellular thiols, especially protein-integrated cysteines, provoked a rapid decrease in cellular glutathione, hence caused oxidative stress. Diamide treatment also activated the PI3K–AKT–mTOR pathway in PC3 cells (Fig. 1G).

Having established that oxidative stress leads to elevation of Plk1 and activation of the PI3K–AKT–mTOR pathway, we next asked whether these two events are interrelated and interdependent. Toward that end, we used lentivirus-based RNAi to deplete Plk1 in different prostate cell lines, and found that depletion of Plk1 caused a reduction of the levels of phospho-AKT (S473) and phospho-S6, either in the absence or presence of oxidative stress, suggesting that Plk1 acts upstream of the PI3K–AKT–mTOR pathway (Fig. 1H and I). As a control, we showed that the short treatment with H_2O_2 did not affect cell-cycle progression, ruling out the possibility oxidative stress–induced elevation of Plk1 might be a secondary effect of cell-cycle arrest (Fig. 1I, right). To further confirm that oxidative stress–induced activation of AKT is Plk1 dependent, we also inhibited the PI3K–AKT–mTOR pathway with various inhibitors, and found that these inhibitors did not affect oxidative stress–induced elevation of Plk1, supporting that the PI3K–AKT–mTOR pathway acts downstream of Plk1 (Fig. 1J). Mechanistically, oxidative stress–induced Plk1 elevation and activation of the PI3K pathway are NF-κB dependent, as addition of pyrrolidine dithiocarbamate, an NF-κB inhibitor, counteracted the effect (Fig. 1K–M). In agreement with that NF-κB is a transcription factor, oxidative stress also results in an elevation of mRNA level of Plk1 (Fig. 1K). Involvement of NF-κB is also supported by its increased phosphorylation upon oxidative stress (Fig. 1L). As a control, we showed that the nuclear localization of NF-κB was increased upon oxidative stress (Fig. 1N). NF-κB, a transcription factor that regulates a spectrum of biologic responses, is activated by a variety of stimuli, such as radiation and oxidative stress (17). Certain cell types, but certainly not all, respond to oxidative stress by upregulation of NF-κB activity. Our data suggest that NF-κB plays a critical role in prostate cells in response to oxidative stress (Fig. 1K–M). How NF-κB affects Plk1 expression has

Published OnlineFirst September 24, 2014; DOI: 10.1158/0008-5472.CAN-14-1916

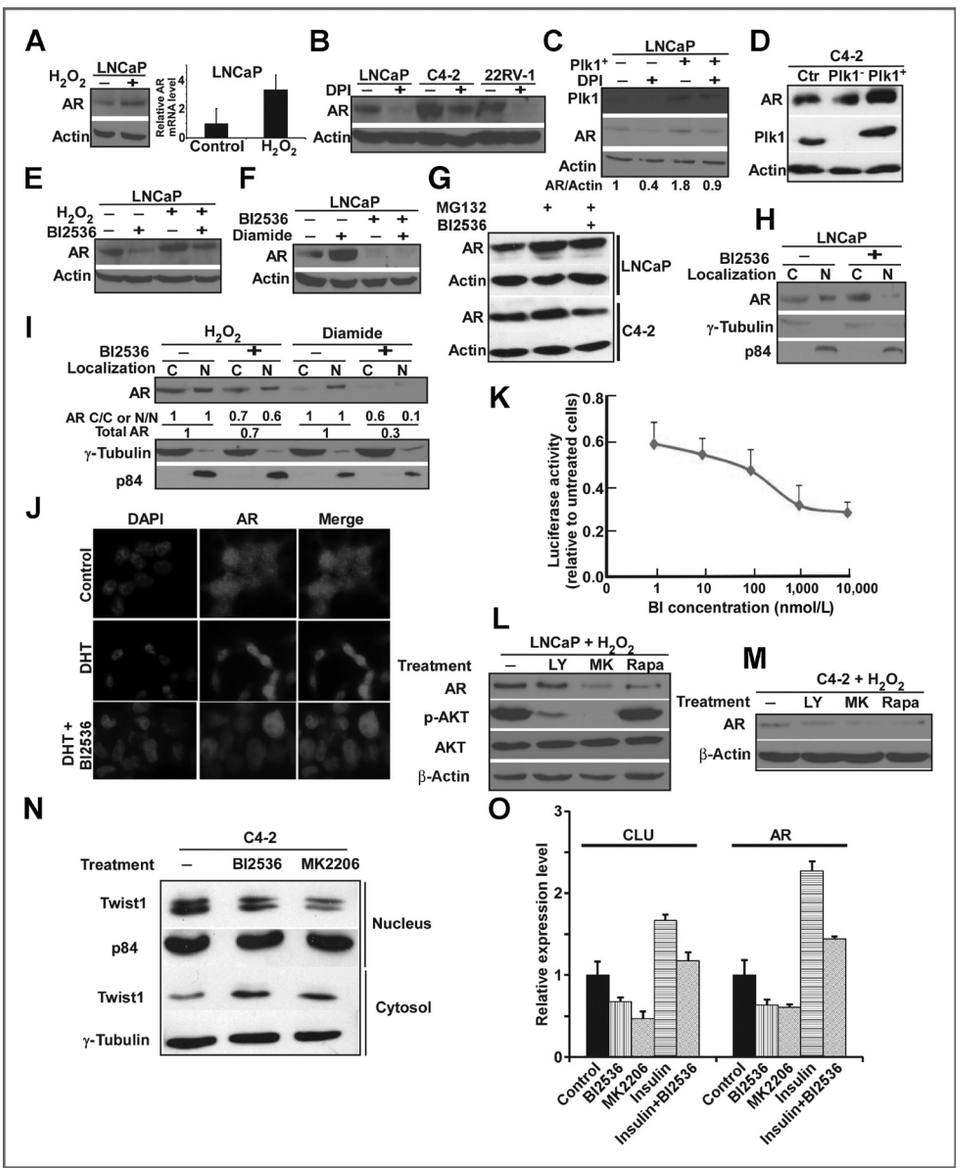

Figure 2. Oxidative stress–induced AR elevation in prostate cancer cells is Plk1 dependent. A, oxidative stress results in elevation of AR level. LNCaP cells were treated with or without 1 mmol/L of H_2O_2 for 5 minutes and harvested for anti-AR immunoblotting or RT-PCR. B, inhibition of oxidative stress reduces AR levels in prostate cancer cells. LNCaP, C4-2, and 22Rv-1 cells were treated with 20 μmol/L of diphenyleneiodonium chloride (DPI) for 24 hours and harvested. C and D, overexpression of Plk1 increases the level of AR protein. C, LNCaP cells were infected with lentivirus that expresses Plk1 for 24 hours, treated with 20 μmol/L DPI for 12 hours, and harvested. D, C4-2 cells were infected with lentivirus to deplete or overexpress Plk1 for 24 hours and harvested. E and F, inhibition of Plk1 prevents oxidative stress–induced elevation of AR protein. LNCaP cells were preincubated with or without 100 nmol/L of BI2536 for 2 hours, treated with 1 mmol/L of H_2O_2 for 5 minutes (E) or 1 mmol/L of diamide for 5 minutes (F), and harvested. G, AR of C4-2 cells are more sensitive to inhibition of Plk1 than AR of LNCaP cells. LNCaP or C4-2 cells were treated with MG132 ± BI2536 and harvested. H, inhibition of Plk1 decreases the level of nuclear AR. After LNCaP cells were treated with 100 nmol/L of BI2536 for 2 hours, lysates were subjected to subcellular fractionation to obtain cytoplasmic (C) and nuclear (N) fractions, followed by anti-AR immunoblotting. Only half of cytoplasmic fractions were loaded because of the limited volumes of gel wells. I, inhibition of Plk1 decreases AR expression under oxidative stress. LNCaP cells were incubated with 100 nmol/L of BI2536 for 8 hours, treated with 1 mmol/L of H_2O_2 or 1 mmol/L of diamide for 5 minutes, and harvested for subcellular fractionation. Cytoplasmic and nuclear fractions were analyzed by anti-AR immunoblotting. Only half of cytoplasmic fractions were loaded because of the limited volumes of gel wells. To quantify, we set the intensities of non-BI2536–treated lanes to be 1.0. J, inhibition of Plk1 decreases nuclear AR intensity. LNCaP cells were preincubated with or without 100 nmol/L of BI2536 for 2 hours, treated with 100 nmol/L of dihydrotestosterone (DHT) for 2 hours, and harvested for anti-AR immunofluorescent staining. K, BI2536 inhibits AR activity. LNCaP cells were treated with different concentrations of BI2536, followed by luciferase assay to measure AR activity. L and M, inhibition of the PI3K–AKT–mTOR pathway antagonizes the oxidative stress–induced activation of AR. LNCaP (L) and C4-2 (M) cells were preincubated with the PI3K–AKT–mTOR pathway inhibitors (25 μmol/L of LY294002 for 1 hour, 5 μmol/L of MK-2206 for 2 hours, or 100 nmol/L of rapamycin for 2 hours), treated with 1 mmol/L of H_2O_2 for 5 minutes, and harvested. N, inhibition of Plk1 and AKT reduced the level of nuclear Twist protein in C4-2 cells. O, BI2536 inhibits Twist1 activity. C4-2 cells were treated with BI2536 (10 nmol/L, 12 hours), MK2206 (20 nmol/L, 6 hours), insulin (1 nmol/L, 6 hours), or BI2536 plus insulin, and harvested for RT-PCR to measure mRNA levels of CLU (clusterin) and AR, two transcription targets of Twist1.

Published OnlineFirst September 24, 2014; DOI: 10.1158/0008-5472.CAN-14-1916

been described previously (18). Plk1 is a transcriptional target of the RelA subunit of NF-κB and upregulation of Plk1 induced by cell detachment is RelA dependent (18). Our finding suggests that NF-κB might be responsible for elevation of Plk1 in CRPC in which the constitutive activation of NF-κB is observed (19).

Oxidative stress induces activation of AR signaling in a Plk1-dependent manner

In addition to the PI3K–AKT–mTOR pathway, continued activation of AR signaling contributes to CRPC. We therefore asked whether oxidative stress leads to activation of AR signaling *in vitro*. Treatment of LNCaP cells with H_2O_2 resulted in elevation of both AR protein and mRNA (Fig. 2A), whereas inhibition of oxidative stress with diphenyleneiodonium chloride led to decreased levels of AR in multiple prostate cancer cell lines, including two CRPC cell lines, C4-2 and 22Rv1 (Fig. 2B), suggesting that oxidative stress is likely one contributing factor that activates AR signaling in CRPC. We then asked whether oxidative stress–associated AR activation is Plk1 dependent with different approaches. Lentivirus-mediated overexpression of Plk1 increased the expression levels of AR in LNCaP cells either in the presence or absence of diphenyleneiodonium chloride (Fig. 2C). Plk1 overexpression led to an increase of AR protein in C4-2 cells as well (Fig. 2D). In agreement, BI2536-mediated inhibition of Plk1 decreased the expression levels of AR in LNCaP cells either in presence or absence of oxidative stress (Fig. 2E and F). We also noticed that AR level of C4-2 cells was much more sensitive to BI2536 than that of LNCaP cells, indicating that Plk1 likely plays a more important role in late-stage prostate cancer (Fig. 2G). Considering that AR is a transcription factor, which has to shuttle into the nucleus to control its downstream targets, we also analyzed its subcellular localization by fractionation upon inhibition of Plk1. As indicated, inhibition of Plk1 by BI2536 led to reduced levels of nuclear AR either in the absence (Fig. 2H) or presence of oxidative stress (Fig. 2I). The reduced levels of nuclear AR upon inhibition of Plk1 under different cellular conditions, such as oxidative stress and dihydrotestosterone treatment, were also confirmed by anti-AR immunofluorescent staining (Fig. 2J). Furthermore, treatment of LNCaP cells with BI2536 inhibited AR transactivation activity in a dose-dependent manner in the AR luciferase assay (Fig. 2K). Because oxidative stress activates both the PI3K–AKT–mTOR pathway and AR signaling, we asked whether these two pathways regulate each other under this condition. As indicated in Fig. 2L and M, treatment of LNCaP and C4-2 cells with various inhibitors of the PI3K–AKT–mTOR pathway significantly antagonized oxidative stress–induced AR activation. Therefore, the PI3K–AKT–mTOR pathway also contributes to AR activation upon oxidative stress. To understand the underlying mechanism of this observation, we turned our attention to Twist1 transcription factor. It was shown that AKT phosphorylation of Twist1 at S42 leads to its activation to promote cell survival during carcinogenesis (20), and that activated Twist1 increases AR expression through binding to E-boxes in AR promoter region upon castration-induced oxidative stress (21). Because Twist1 is an important mediator between AKT and AR, we asked whether inhibition of Plk1 affects the nuclear accumulation of Twist1. As indicated, treatment of C4-2 cells with both BI2536 and MK2206 led to an obvious reduction of nuclear Twist1 protein level (Fig. 2N). Of interest, the cytosolic fraction of Twist1 was apparently increased upon treatment with BI2536 and MK2206 (Fig. 2N), suggesting that it is the nuclear localization of Twist1 that is regulated by Plk1 and AKT. Finally, BI2536 treatment clearly inhibited insulin-induced transcription of CLU and AR, two Twsit1 targets (Fig. 2O), in agreement with a reduced protein level of nuclear Twist1 (Fig. 2N).

Plk1 affects cholesterol metabolism in prostate cancer cells via the SREBP pathway

To confirm that Plk1 regulates AR signaling, we then analyzed the status of the SREBP pathway upon inhibition of Plk1 with BI2536. Treatment of LNCaP and C4-2 cells with BI2536 led to reduced levels of cleaved forms of SREBP2 (Fig. 3A) and SREBP1 (Fig. 3B). To ask whether this observation is limited to AR-positive cells, we also performed a series of Western blot analyses with antibodies against SREBP1/2 in PC3 and DU145 cells. Inhibition of Plk1 with BI2536 also reduced the expression levels of cleaved forms of SREBP2 (Fig. 3C) and SREBP1 (Fig. 3D) in PC3 and DU145 cells, suggesting that BI2536-induced downregulation of the SREBP pathway is likely a general phenomenon in prostate cancer. To further confirm this, we tested whether inhibition of Plk1 affects the downstream targets of SREBP. As indicated in Fig. 3E, BI2536 treatment led to reduced transcription levels of FAS, mevalonate kinase (MVK), and 3-hydroxy-3-methyl-glutaryl-CoA reductase (HMGCR), three targets of SREBP, supported by decreased levels of proteins upon BI2536 treatment (Fig. 3F). Of note, 4-hour treatment with BI2536 is enough for us to detect significant reductions of these genes in C4-2 cells, whereas 24 hours are needed to observe an apparent inhibition in LNCaP cells (Fig. 3E), suggesting that androgen-independent C4-2 cells are much more sensitive to BI2536 than androgen-dependent LNCaP cells. Considering that SREBP is also regulated by the Fbw7–GSK3β pathway and that AKT-associated phosphorylation suppresses GSK3β, we thus tested whether BI2536 also affects the activation of GSK3β. As indicated in Fig. 3G, inhibition of Plk1 also reduced phosphorylation level of GSK3β, suggesting that the AKT–GSK3β axis might be also involved in Plk1-dependent activation of the SREBP pathway. Furthermore, to answer the question whether a general decay of cellular protein is the cause for reduced AR and FAS levels following BI2536 treatment, we performed a time-course experiment in which an apoptosis analysis was included. BI2536 treatment led to reduced levels of AR and FAS after 8 hours of incubation, but cell death was not detected until 12 hours, ruling out the possibility that Plk1 inhibition-induced reduction of AR and FAS levels in LNCaP cells is a secondary effect of cell death (Fig. 3H). For C4-2 cells, as short as 4 hours of BI2536 treatment is enough for us to detect apparent reduction of AR and FAS levels.

Using a stimulated Raman scattering microscope, we recently reported that the high-grade prostate cancer tissues

Published OnlineFirst September 24, 2014; DOI: 10.1158/0008-5472.CAN-14-1916

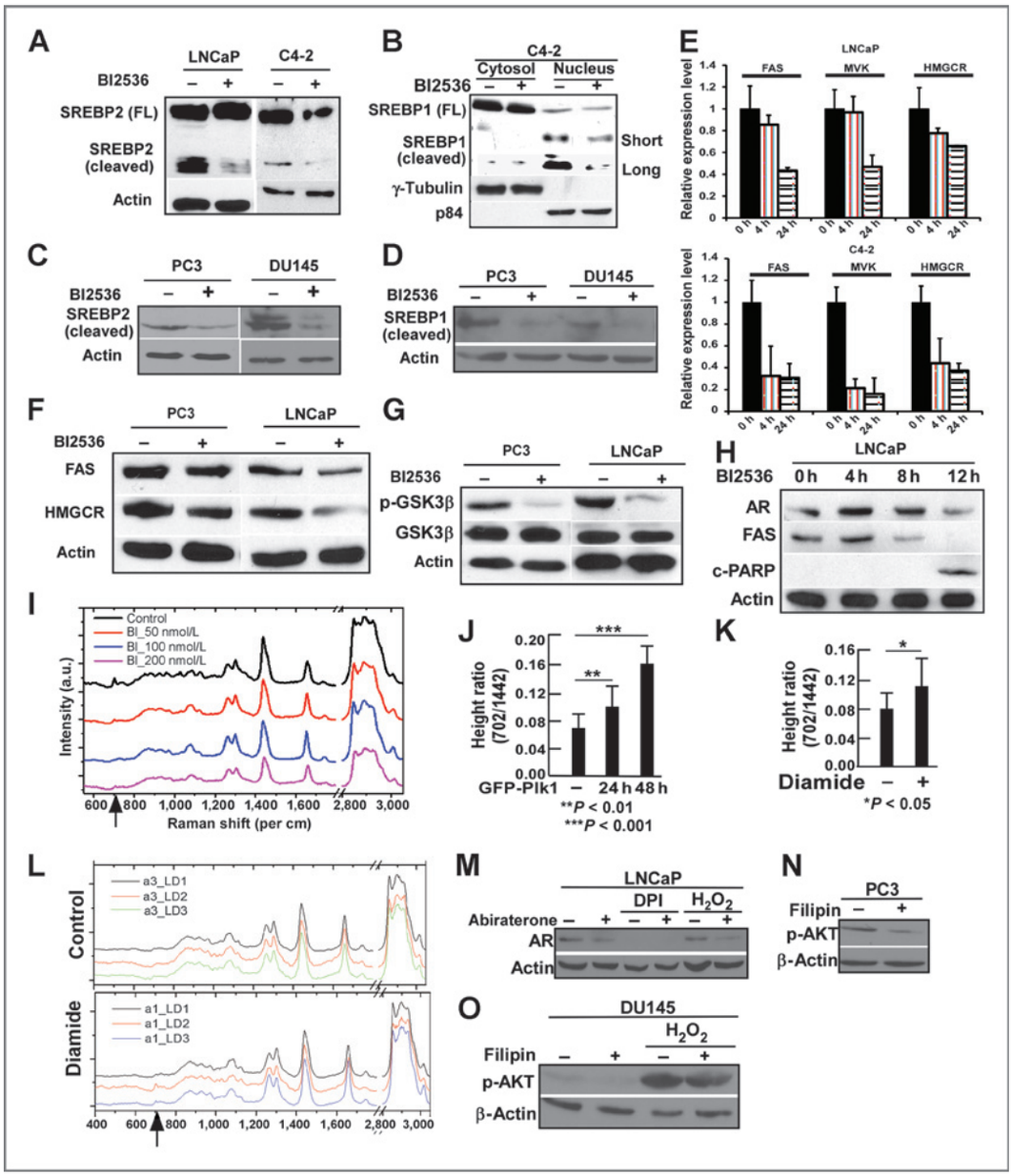

Figure 3. Plk1 affects lipid metabolism in prostate cancer. A, inhibition of Plk1 reduces the active (cleaved) form of SREBP2. LNCaP and C4-2 cells were treated with BI2536 and harvested for immunoblotting. B, inhibition of Plk1 reduces the active (cleaved) form of SREBP1. C4-2 cells were treated with BI2536, followed by subcellular fractionation. C and D, inhibition of Plk1 decreases the protein levels of active forms of SREBP1/2 in PC3 and DU145 cells. Cells were treated with or without 100 nmol/L of BI2536 for 12 hours and harvested for immunoblotting with antibodies against SREBP2 (C) or SREBP1 (D). E and F, BI2536 inhibits the SREBP pathway. E, LNCaP (top) and C4-2 (bottom) cells were treated with 10nmol/L BI2536 for 4 or 24 hours and harvested for real-time qPCR to measure the mRNA levels of three SREBP-regulated genes. F, PC3 and LNCaP cells were treated with BI2536 and harvested for immunoblotting. G, BI2536 inhibits phosphorylation of GSK3β. Cells were treated with BI2536 and harvested. H, Plk1 inhibition-induced reduction of AR and FAS levels occurs before massive apoptosis. LNCaP cells were treated with BI2536 for different time and harvested for immunoblotting. I, inhibition of Plk1 blocks the accumulation of CE in PC3 cells. PC3 cells were treated with different concentrations of BI2536 for 60 hours and subjected to Raman microscopic analysis. The arrow at bottom indicates the 702 per cm peak due to cholesterol ring vibration. J, overexpression of Plk1 increases CE accumulation. PC3 cells were infected with GFP-Plk1–expressing lentivirus for 24 or 48 hours and subjected to Raman microscopic analysis. The ratio of intensity of the CE peak 702 per cm versus intensity of the peak 1442 per cm in each cell was calculated. Ten cells from each group were randomly selected for CE measurement. K and L, oxidative stress increases CE accumulation. LNCaP cells were treated with or without 1 mmol/L of diamide for 5 minutes and subjected to Raman microscopic analysis. Ten cells from each group were randomly chosen to calculate the ratio of intensity of the CE peak 702 per cm versus intensity of the peak 1442 per cm in each cell. M, inhibition of steroidogenesis antagonizes oxidative stress–induced AR elevation. LNCaP cells, growing in RPMI-1640 medium with 5% charcoal-stripped FBS, were preincubated with 1 μmol/L of abiraterone for 24 hours, treated with 20 μmol/L of diphenyleneiodonium chloride (DPI) for 12 hours or 1 mmol/L of H_2O_2 for 5 minutes, and harvested for anti-AR immunoblotting. N and O, inhibition of lipid rafts decreases activation of AKT. PC3 (N) or DU145 (O) cells were preincubated with 2 μg/mL of filipin for 1 hour, treated with 1 mmol/L of H_2O_2 for 5 minutes, and harvested for anti-p-AKT immunoblotting.

Published OnlineFirst September 24, 2014; DOI: 10.1158/0008-5472.CAN-14-1916

contained significantly more CE than the low-grade ones, suggesting an important correlation of CE accumulation with prostate cancer progression (8). Of significance, inhibition of Plk1 reduced the level of CE in PC3 cells in a concentration-dependent manner (Fig. 3I), suggesting that Plk1 acts upstream of cholesterol synthesis during prostate cancer progression. In support, lentivirus-mediated overexpression of Plk1 increased CE accumulation in PC3 cells (Fig. 3J), confirming that Plk1 acts upstream of cholesterol biosynthesis in prostate cancer progression. We next asked whether oxidative stress affects CE accumulation in prostate cancer. As expected, diamide treatment increased the level of CE in PC3 cells (Fig. 3K and L). Because Plk1-associated kinase activity affects cholesterol metabolism and because cholesterol is the precursor of androgen during *de novo* steroidogenesis, we asked whether there is a positive feedback loop between AR signaling and cholesterol biosynthesis (Fig. 7). In other words, Plk1-mediated activation of AR signaling increases cholesterol biosynthesis via the SREBP pathway, and elevation of cholesterol levels further activates AR signaling via *de novo* androgen biosynthesis. As indicated, treatment with abiraterone, an inhibitor of androgen biosynthesis, prevented oxidative stress–induced activation of AR signaling, suggesting a positive feedback loop (Fig. 3M). For the similar reason, we also asked whether there is another positive feedback loop between the PI3K–AKT–mTOR pathway and lipid synthesis (Fig. 7). In other words, Plk1-mediated activation of the PI3K–AKT–mTOR pathway increases lipid synthesis via the SREBP pathway, and elevation of fatty acid and cholesterol levels further activates the PI3K–AKT–mTOR pathway in lipid rafts. As indicated, treatment with the lipid raft–disrupting agent, filipin, a polyene macrolide that binds cholesterol with high specificity, reduced oxidative stress–induced activation of AKT, supporting a positive feedback loop as well (Fig. 3N and O).

AR positively regulates Plk1

Given that AR is a transfection factor, we also asked whether AR regulates the level of Plk1. As indicated, AR expression in PC3 and 293T cells led to elevation of Plk1 transcription (Fig. 4A) and AR depletion in LNCaP and C4-2 cells resulted in reduction of Plk1 protein (Fig. 4B). We acknowledge that recent evidence suggests that AR-vs that lack the functional ligand-binding domain (LBD) also play important roles in resistance to ASI in CRPC (22–24). AR-vs originate from AR transcripts with insertions of cryptic exons downstream of the coding sequences for AR DNA-binding domain (e.g., AR-v7) or with deletions of exons coding for AR-LBD (e.g., AR-v567es). Microarray data show that AR-WT and AR-vs mediate distinctive transcriptional programs, as AR-vs preferentially induce elevation of cell-cycle genes, including Plk1 (22). Thus, we asked whether depletion of AR-vs affects the level of Plk1. As indicated, depletion of both AR-V7 and AR-V1 caused obvious reduction of the levels of Plk1 protein (Fig. 4C, top) and mRNA (Fig. 4C, bottom).

Inhibition of Plk1 potentiates the effect of ASI

Because Plk1 elevation leads to constitutive activation of AR, the major mechanism for development of resistance of ASI, we performed a series of experiments to ask whether ASI and BI2536 inhibit AR signaling in CRPC cells in a synergistic manner. A combination of low concentrations of abiraterone and BI2536 resulted in a much more dramatic reduction of protein levels of AR-WT in C4-2 (Fig. 4D) and AR-vs in 22Rv1 cells (Fig. 4E). Moreover, a combination of low concentrations of enzalutamide (MDV3100) and BI2536 also led to a more significant reduction of AR-WT in C4-2 (Fig. 4F) and AR-vs in 22Rv1 cells (Fig. 4G). Of note, elevation of AR-vs has been reported to contribute to resistance to inhibition of AR signaling in CRPC (23, 24). Thus, the data in Fig. 4E and G suggest that a combination of BI2536 and ASI could be a novel avenue to overcome ASI-resistance due to elevation of AR-vs. Next, we performed fluorescence-activated cell sorting (FACS) analysis to follow any cell-cycle defect upon drug treatment. As indicated, the presence of enzalutamide potentiated BI2536-induced G_2–M arrest in 22Rv1 cells (Fig. 4H). Furthermore, a combination of BI2536 and enzalutamide strongly antagonized R1881-induced nuclear accumulation of AR in LNCaP cells (Fig. 4I). We also asked whether BI2536 and enzalutamide act synergistically in LNCaP cells by measuring the combination index (CI) with the following equation: $CI = (Am)_{50}/(As)_{50} + (Bm)_{50}/(Bs)_{50}$, where $(Am)_{50}$ is the IC_{50} of drug A in the combination, $(As)_{50}$ is the concentration of drug A that will produce the identical level of effect alone, $(Bm)_{50}$ is the IC_{50} of drug B in the combination, and $(Bs)_{50}$ is the IC_{50} of drug B after single administration. Antagonism is indicated when $CI > 1$, $CI = 1$ indicates an additive effect, and $CI < 1$ indicates synergy. Our calculations led to a CI value of 0.12, suggesting that BI2536 and enzalutamide act synergistically to induce apoptosis (Fig. 4J). Finally, androgen treatment of LNCaP cells growing in charcoal stripped fetal bovine serum (CSS) medium apparently stimulated Plk1 expression, and enzalutamide treatment of LNCaP cells culturing in normal medium inhibited the expression level of Plk1, further confirming that Plk1 is an AR target (Fig. 4K).

Inhibition of Plk1 overcomes ASI resistance

Next, we treated MR49F cells, the enzalutamide-resistant LNCaP cells (25), with enzalutamide and BI2536 and found that MR49F cells became much more sensitive to enzalutamide in the presence of BI2536, indicated by an almost complete disappearance of AR protein and a huge increase of c-PARP (Fig. 5A and B). Furthermore, treatment with BI2536 plus enzalutamide led to a much stronger G_2–M arrest and androgen-induced AR nuclear localization than monotherapy in MR49F cells (Fig. 5C and D). Finally, the castration-resistant LuCaP35CR xenograft tumors, directly derived from human patients with CRPC (24), were used to test the efficacy of the combination of BI2536 and abiraterone. As indicated, the combination of BI2536 and abiraterone almost completely blocked tumor growth and elevation of serum PSA. In striking contrast, monotherapies with low concentrations of BI2536 or abiraterone did not significantly affect tumor growth and serum PSA levels (Fig. 6A–D). To support our cell culture–based data, the levels of testosterone, the precursor of dihydrotestosterone, were reduced in

Published OnlineFirst September 24, 2014; DOI: 10.1158/0008-5472.CAN-14-1916

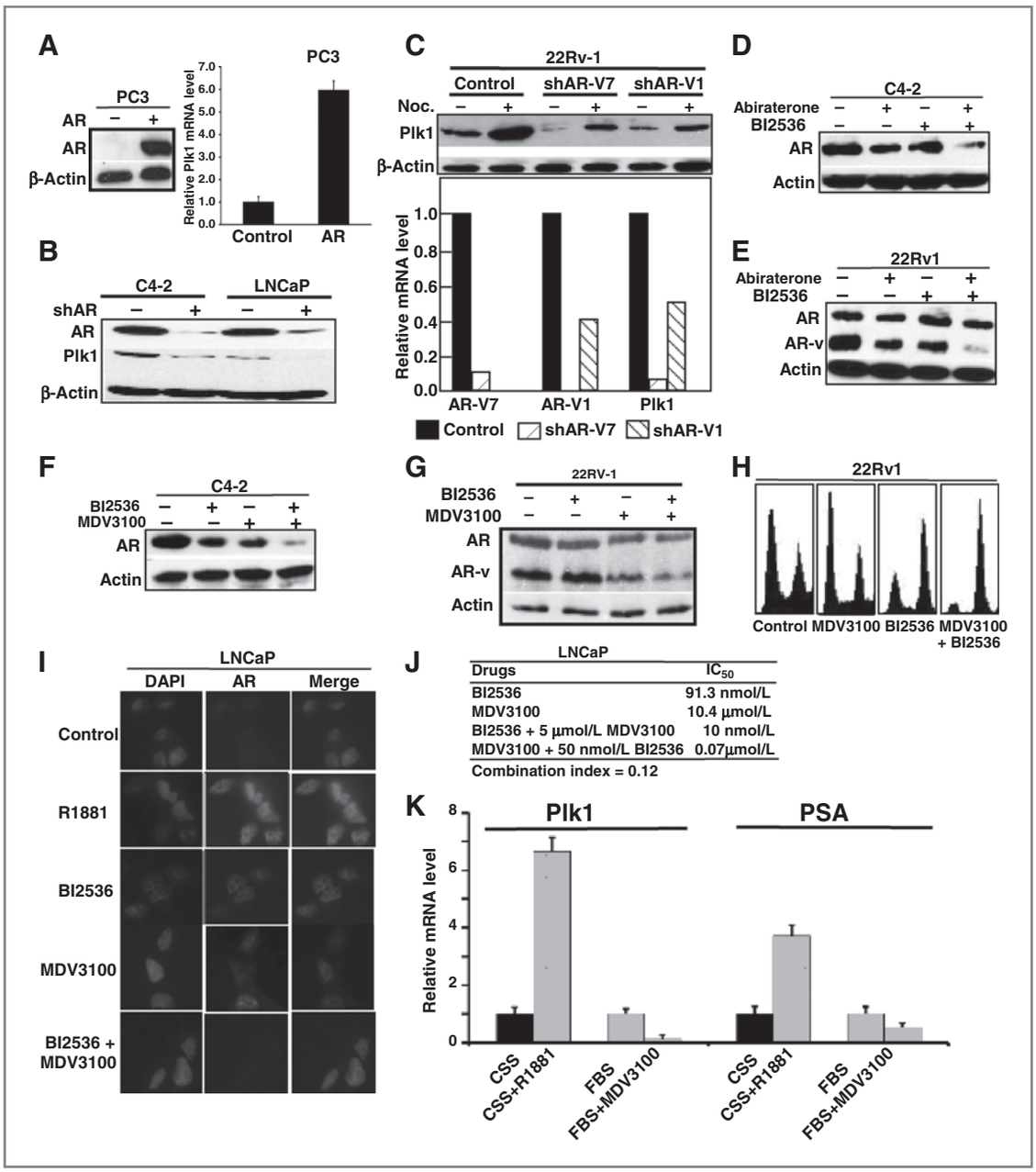

Figure 4. Inhibition of Plk1 enhances cellular response to ASI in prostate cancer cells. A–C, AR and AR-vs regulate Plk1. A, expression of AR increases the level of Plk1 in AR-null cells. PC3 cells were transfected with AR and harvested for RT-PCR. B, depletion of AR reduces the levels of Plk1 in AR-positive cells. LNCaP or C4-2 cells were transfected with shRNA to deplete AR and harvested for immunoblotting. C, depletion of AR-vs reduces the level of Plk1. 22Rv-1 cells were transfected with shRNA to deplete AR-v1 or AR-v7, treated with nocodazole, and harvested for immunoblotting (top) or RT-PCR (bottom). D and E, BI2536 and abiraterone inhibit AR signaling in a synergistic manner. C4-2 (D) and 22Rv1 (E) CRPC cells were treated with BI2536 (10 nmol/L), abiraterone (10 μmol/L) or both for 24 hours, and harvested for immunoblotting. F–H, BI2536 and enzalutamide inhibit AR signaling synergistically. C4-2 (F) and 22Rv1 (G and H) cells were treated with BI2536 (10 nmol/L), enzalutamide (10 μmol/L), or both for 24 hours, and harvested for immunoblotting (F and G) or FACS (H). I, LNCaP cells were treated with BI2536 (10 nmol/L), enzalutamide (10 μmol/L), or both for 24 hours, then treated with R1881 for 2 hours, and harvested for anti-AR immunofluorescent staining. J, the CI of BI2536 and enzalutamide in LNCaP cells. K, Plk1 transcription is regulated by AR signaling. LNCaP cells were grown in different conditions (CSS media and treated with R1881 or FBS-containing media and treated with MDV3100) and harvested for RT-PCR.

both BI2536 and abiraterone-treated tumors. A combination of BI2536 and abiraterone led to the most significant inhibition of the level of testosterone (Fig. 6E). Consistent with these mass spectrometry–based measurements, lipid droplets in the LuCaP35CR tumors were dramatically reduced upon BI2536 treatment (Fig. 6F). Of note, we recently

Published OnlineFirst September 24, 2014; DOI: 10.1158/0008-5472.CAN-14-1916

reported that the major component of lipid droplets in prostate cancer was found to be CE (26).

Discussion

Oxidative stress in prostate cancer

Evidence from both experimental and clinical studies suggests that prostate cancer cells are exposed to increased oxidative stress (2, 27). Indeed, it has been demonstrated that oxidative stress is inherent in prostate cancer cells (28). Therefore, understanding how ROS regulate cellular processes controlling transformation during the progression of prostate cancer will open doors for the development of novel therapeutics for prostate cancer (2). In particular, castration, the major approach for treatment of late-stage prostate cancer (29), significantly increases oxidative stress of the prostate (21, 27, 30). However, whether and how castration-induced oxidative stress contributes to CRPC is still elusive. Herein, we provide evidence to show that oxidative stress led to activation of the PI3K–AKT–mTOR pathway (Fig. 1), activation of AR signaling (Fig. 2), and elevation of cholesterol biosynthesis (Fig. 3), three hallmarks of CRPC. Of note, Plk1 turns out to be a critical molecule that links all these prostate cancer–specific signaling pathways. We understand that 1 mmol/L H_2O_2 treatment might not be physiologic relevance. We initially chose such treatment, as used previously (31), to establish a link among oxidative stress, Plk1, and signaling pathways that are involved in prostate cancer. Additional experiments without H_2O_2 treatment further confirmed that Plk1-associated kinase activity activates these pathways is a general phenomenon.

ASI in CRPC treatment

CRPC remains an incurable disease today. AR antagonists, such as bicalutamide and nilutamide, have been used in CRPC for three decades. Unfortunately, the duration of response to these anti-androgens is often less than 4 months; their AR binding is reversible, and paradoxical agonism of the AR occurs in 10% to 15% of patients (32). Two most recently FDA-approved drugs to treat CRPC are abiraterone and enzalutamide, which improve overall survival for 5 and 2 months, respectively (4, 5). Although abiraterone acetate blocks *de novo* androgen biosynthesis from cholesterol, enzalutamide is a direct AR inhibitor. On the basis of mutual regulation of Plk1 and AR, we hypothesized that inhibition of Plk1 might be a novel approach to overcome resistance to ASI (Fig. 7). Both cell culture–based *in vitro* assays and patient-derived xenograft tumor experiments led to the conclusion that inhibition of Plk1 significantly enhanced the efficacy of ASI in CRPC. Because BI2536 has been well tolerated by patients in clinical trials, and because we used much lower concentrations of BI2536 and ASI than the previous publications, the data presented here support an immediate clinical trial with a combination of BI2536 and ASI to improve the treatment of CRPC.

Plk1 in drug resistance

Increasing evidence suggests that Plk1 has many nonmitotic functions. In particular, Plk1 is significantly elevated in interphase of transformed cells, but not in normal cells, suggesting that Plk1 must have cancer cell–specific functions (33). In support, elevation of Plk1 leads to inactivation of tumor-suppressor p53 via its kinase activity toward GTSE1 and Topors, two negative regulators of p53 (34, 35). Because many chemotherapeutic drugs, such as doxorubicin, act via p53-dependent cell-cycle arrest and apoptosis, Plk1 elevation has been proposed to contribute to development of

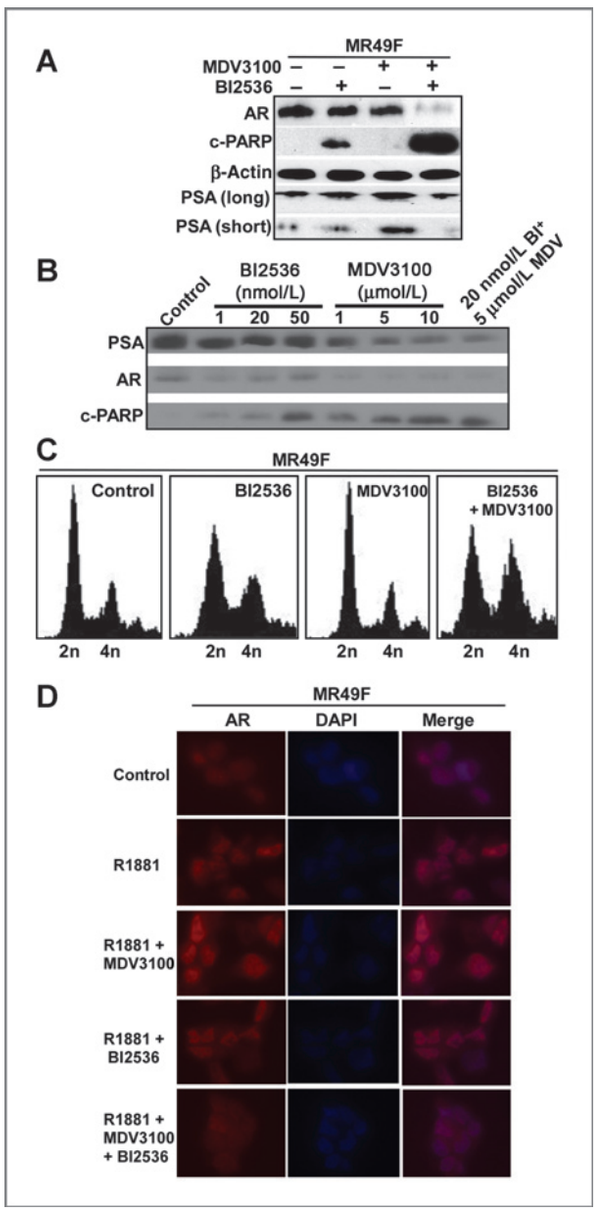

Figure 5. Inhibition of Plk1 sensitizes MR49F cells to enzalutamide. A, MR49F cells were treated with BI2536 (10 nmol/L), enzalutamide (10 μmol/L), or both for 24 hours, and harvested for immunoblotting. B, MR49F cells were treated with indicated concentrations of BI2536 and enzalutamide. C, cells in A were harvested for FACS analysis. D, MR49F cells as in A were treated with R1881 for 2 hours and harvested for anti-AR immunofluorescent staining.

Published OnlineFirst September 24, 2014; DOI: 10.1158/0008-5472.CAN-14-1916

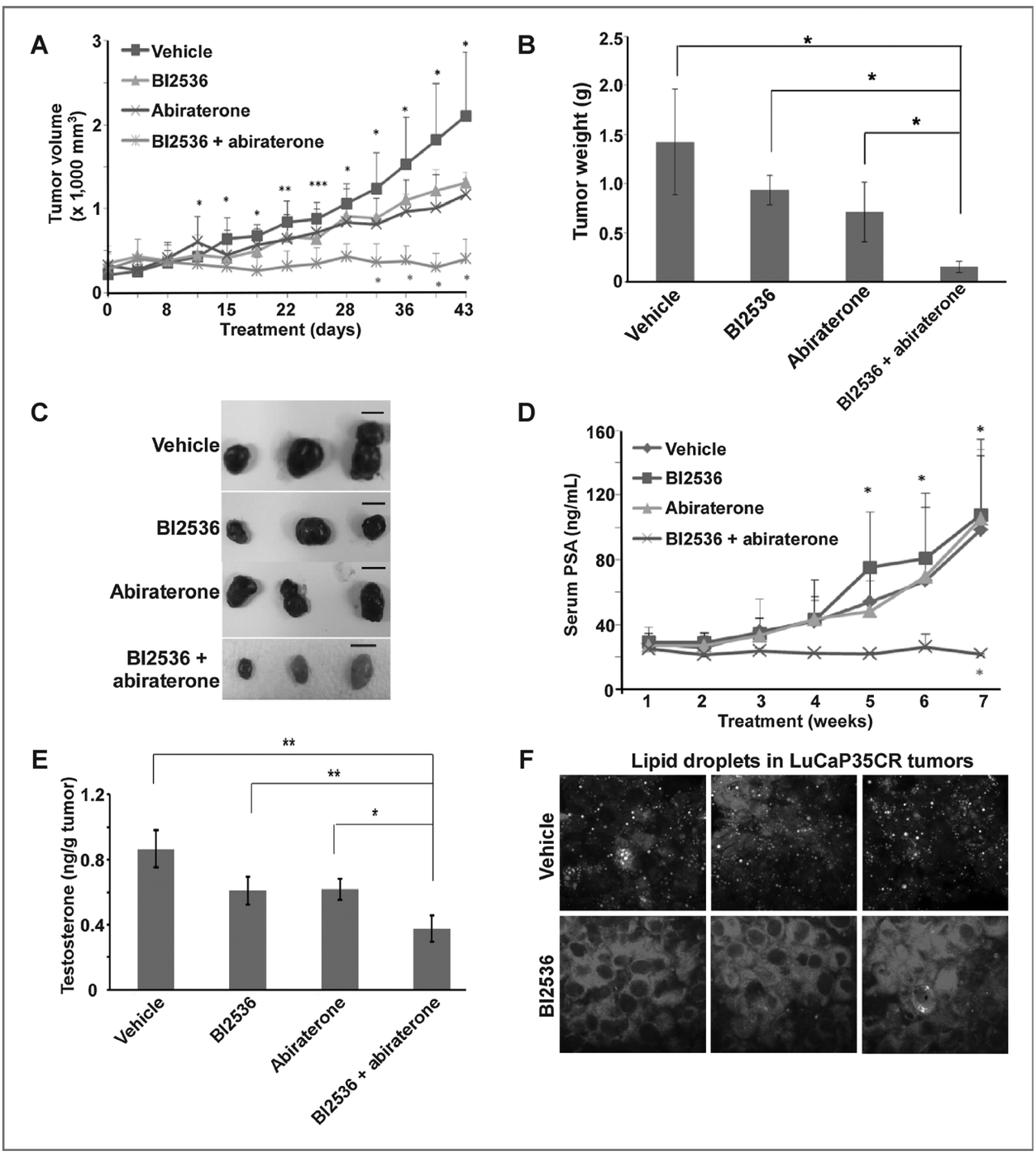

Figure 6. BI2536 and abiraterone inhibit LuCaP35CR xenografts synergistically. LuCaP35CR tumors were inoculated into nude mice, which had been castrated 2 weeks ahead. After waiting for several weeks for tumors to reach 250 to 300 mm^3, mice were intravenously injected twice per week with BI2536 (10 mg/kg), abiraterone (50 mg/kg), or both, and followed for additional 43 days. A, tumor growth curves of the study. B, tumor weight measurement after being freshly removed from the bodies. C, images of the mice at the end of the study. D, inhibition of PSA level by BI2536 and abiraterone. Blood was collected once a week and serum PSA level was measured using the PSA ELISA Kit. E, The levels of testosterone were measured by mass spectrometry as described previously (43). F, the levels of lipid droplets in LuCaP35CR tumors were measured by label-free Raman spectromicroscopy as described previously (8).

chemoresistance. Plk1 phosphorylation of CLIP-170 and $p150^{Glued}$, two microtubule plus-end binding proteins, led to increased microtubule dynamics, thus reducing the efficacy of taxol, an inhibitor of tubulin depolymerization (36–38). We also showed that Plk1 phosphorylation of Orc2 and Hbo1, two members of DNA replication machinery,

Published OnlineFirst September 24, 2014; DOI: 10.1158/0008-5472.CAN-14-1916

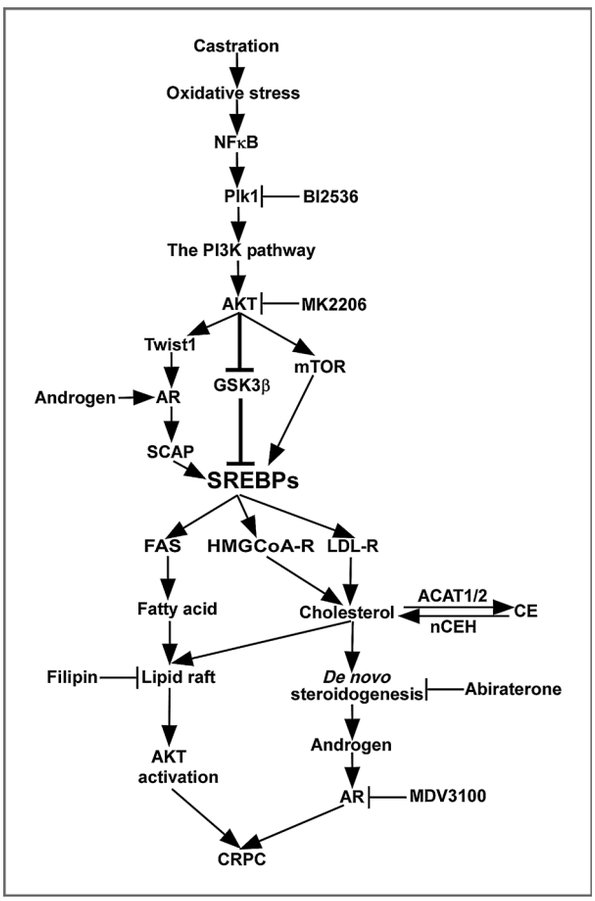

Figure 7. A proposed working model. The level of cholesterol is regulated by (i) homoeostasis by SREBP-1/2, (ii) neosynthesis by HMGCoA-R; (iii) uptake by LDL-R; (iv) esterification by ACAT; and (v) CE hydrolysis by nCEH. ACAT, acyl-CoA:cholesterol acyltransferase; nCEH, neutral CE hydrolase.

increased DNA replication in the presence of replication stress, eventually contributing to development of resistance to additional chemotherapeutic drugs that cause DNA replication stress such as gemcitabine (39–41). The data presented here demonstrated that Plk1 also plays a critical role in cellular response to ASI and that inhibition of Plk1 overcomes ASI resistance in CRPC. Although how Plk1 elevation leads to activation of AR signaling and elevation of cholesterol biosynthesis are currently under heavy investigation in the Liu laboratory, we recently reported one mechanism that is responsible for Plk1-dependent activation of the PI3K–AKT–mTOR pathway. We showed that Plk1 phosphorylation of PTEN-S385 leads to its inactivation, thus activation of the PI3K–AKT–mTOR pathway (42).

Disclosure of Potential Conflicts of Interest

No potential conflicts of interest are disclosed by the authors.

Authors' Contributions

Conception and design: Z. Zhang, C. Shao, T. Ratliff, X. Liu
Development of methodology: Z. Zhang, X. Hou, C. Shao, J.-X. Cheng
Acquisition of data (provided animals, acquired and managed patients, provided facilities, etc.): Z. Zhang, X. Hou, C. Shao, J. Li, S. Kuang
Analysis and interpretation of data (e.g., statistical analysis, biostatistics, computational analysis): Z. Zhang, X. Hou, J. Li, X. Liu
Writing, review, and/or revision of the manuscript: Z. Zhang, J. Li, N. Ahmad, X. Liu
Administrative, technical, or material support (i.e., reporting or organizing data, constructing databases): Z. Zhang, X. Hou, S. Kuang, T. Ratliff, X. Liu
Study supervision: Z. Zhang, X. Liu

Acknowledgments

The authors thank Dr. Amina Zoubeidi for MR49F cells and Dr. Robert Vessella for the LuCaP35CR mouse line.

Grant Support

This work was supported by NIH grant R01 CA157429 (X. Liu), NIH grant R01 AR059130 (N. Ahmad), NSF grant MCB-1049693 (X. Liu), and ACS grant RSG-13-073 (X. Liu). Z. Zhang, X. Hou, and C. Shao were financially supported by China Scholarship Council (CSC). Xenograft data were acquired by a Purdue Center for Cancer Research facility supported by P30 CA023168 and support for this publication was made possible by P30 CA023168.

The costs of publication of this article were defrayed in part by the payment of page charges. This article must therefore be hereby marked *advertisement* in accordance with 18 U.S.C. Section 1734 solely to indicate this fact.

Received June 27, 2014; revised September 2, 2014; accepted September 8, 2014; published OnlineFirst September 24, 2014.

References

1. Siegel R, Ma J, Zou Z, Jemal A. Cancer statistics, 2014. CA Cancer J Clin 2014;64:9–29.
2. Khandrika L, Kumar B, Koul S, Maroni P, Koul HK. Oxidative stress in prostate cancer. Cancer Lett 2009;282:125–36.
3. Saad F. Evidence for the efficacy of enzalutamide in postchemotherapy metastatic castrate-resistant prostate cancer. Ther Adv Urol 2013;5:201–10.
4. Beer TM, Armstrong AJ, Rathkopf DE, Loriot Y, Sternberg CN, Higano CS, et al. Enzalutamide in metastatic prostate cancer before chemotherapy. N Engl J Med 2014;371:424–33.
5. Rathkopf DE, Smith MR, de Bono JS, Logothetis CJ, Shore ND, de Souza P, et al. Updated interim efficacy analysis and long-term safety of abiraterone acetate in metastatic castration-resistant prostate cancer patients without prior chemotherapy (COU-AA-302). Eur Urol 2014; pii: S0302-2838(14)00185-7.
6. Ryan CJ, Molina A, Griffin T. Abiraterone in metastatic prostate cancer. N Engl J Med 2013;368:1458–9.
7. Trotman LC, Niki M, Dotan ZA, Koutcher JA, Di Cristofano A, Xiao A, et al. Pten dose dictates cancer progression in the prostate. PLoS Biol 2003;1:E59.
8. Yue S, Li J, Lee SY, Lee HJ, Shao T, Song B, et al. Cholesteryl ester accumulation induced by PTEN loss and PI3K/AKT activation underlies human prostate cancer aggressiveness. Cell Metab 2014;19:393–406.
9. Yang T, Espenshade PJ, Wright ME, Yabe D, Gong Y, Aebersold R, et al. Crucial step in cholesterol homeostasis: sterols promote binding of SCAP to INSIG-1, a membrane protein that facilitates retention of SREBPs in ER. Cell 2002;110:489–500.
10. Peterson TR, Sengupta SS, Harris TE, Carmack AE, Kang SA, Balderas E, et al. mTOR complex 1 regulates lipin 1 localization to control the SREBP pathway. Cell 2011;146:408–20.
11. Huang WC, Li X, Liu J, Lin J, Chung LW. Activation of androgen receptor, lipogenesis, and oxidative stress converged by SREBP-1 is responsible for regulating growth and progression of prostate cancer cells. Mol Cancer Res 2012;10:133–42.

Published OnlineFirst September 24, 2014; DOI: 10.1158/0008-5472.CAN-14-1916

12. Page ST, Lin DW, Mostaghel EA, Marck BT, Wright JL, Wu J, et al. Dihydrotestosterone administration does not increase intraprostatic androgen concentrations or alter prostate androgen action in healthy men: a randomized-controlled trial. J Clin Endocrinol Metab 2011;96: 430–7.
13. Strebhardt K. Multifaceted polo-like kinases: drug targets and anti-targets for cancer therapy. Nat Rev Drug Discov 2010;9:643–60.
14. Liu XS, Song B, Elzey BD, Ratliff TL, Konieczny SF, Cheng L, et al. Polo-like kinase 1 facilitates loss of Pten tumor suppressor-induced prostate cancer formation. J Biol Chem 2011;286:35795–800.
15. Sun Y, Wang BE, Leong KG, Yue P, Li L, Jhunjhunwala S, et al. Androgen deprivation causes epithelial–mesenchymal transition in the prostate: implications for androgen-deprivation therapy. Cancer Res 2012;72:527–36.
16. Corey E, Quinn JE, Buhler KR, Nelson PS, Macoska JA, True LD, et al. LuCaP 35: a new model of prostate cancer progression to androgen independence. Prostate 2003;55:239–46.
17. Wang T, Zhang X, Li JJ. The role of NF-kappaB in the regulation of cell stress responses. Int Immunopharmacol 2002;2:1509–20.
18. Lin DC, Zhang Y, Pan QJ, Yang H, Shi ZZ, Xie ZH, Wang BS, et al. PLK1 Is transcriptionally activated by NF-kappaB during cell detachment and enhances anoikis resistance through inhibiting beta-catenin degradation in esophageal squamous cell carcinoma. Clin Cancer Res 2011;17:4285–95.
19. Gasparian AV, Yao YJ, Kowalczyk D, Lyakh LA, Karseladze A, Slaga TJ, et al. The role of IKK in constitutive activation of NF-kappaB transcription factor in prostate carcinoma cells. J Cell Sci 2002;115: 141–51.
20. Vichalkovski A, Gresko E, Hess D, Restuccia DF, Hemmings BA. PKB/AKT phosphorylation of the transcription factor Twist-1 at Ser42 inhibits p53 activity in response to DNA damage. Oncogene 2010; 29:3554–65.
21. Shiota M, Yokomizo A, Tada Y, Inokuchi J, Kashiwagi E, Masubuchi D, et al. Castration resistance of prostate cancer cells caused by castration-induced oxidative stress through Twist1 and androgen receptor overexpression. Oncogene 2010;29:237–50.
22. Hu R, Lu C, Mostaghel EA, Yegnasubramanian S, Gurel M, Tannahill C, et al. Distinct transcriptional programs mediated by the ligand-dependent full-length androgen receptor and its splice variants in castration-resistant prostate cancer. Cancer Res 2012;72:3457–62.
23. Li Y, Chan SC, Brand LJ, Hwang TH, Silverstein KA, Dehm SM. Androgen receptor splice variants mediate enzalutamide resistance in castration-resistant prostate cancer cell lines. Cancer Res 2013;73: 483–9.
24. Mostaghel EA, Marck BT, Plymate SR, Vessella RL, Balk S, Matsumoto AM, et al. Resistance to CYP17A1 inhibition with abiraterone in castration-resistant prostate cancer: induction of steroidogenesis and androgen receptor splice variants. Clin Cancer Res 2011;17: 5913–25.
25. Kuruma H, Matsumoto H, Shiota M, Bishop J, Lamoureux F, Thomas C, et al. A novel antiandrogen, compound 30, suppresses castration-resistant and MDV3100-resistant prostate cancer growth *in vitro* and *in vivo*. Mol Cancer Ther 2013;12:567–76.
26. Yue S, Cardenas-Mora JM, Chaboub LS, Lelievre SA, Cheng JX. Label-free analysis of breast tissue polarity by Raman imaging of lipid phase. Biophys J 2012;102:1215–23.
27. Shiota M, Yokomizo A, Naito S. Oxidative stress and androgen receptor signaling in the development and progression of castration-resistant prostate cancer. Free Radic Biol Med 2011;51: 1320–8.
28. Kumar B, Koul S, Khandrika L, Meacham RB, Koul HK. Oxidative stress is inherent in prostate cancer cells and is required for aggressive phenotype. Cancer Res 2008;68:1777–85.
29. Leibowitz-Amit R, Joshua AM. Targeting the androgen receptor in the management of castration-resistant prostate cancer: rationale, progress, and future directions. Curr Oncol 2012;19:S22–31.
30. Tam NN, Gao Y, Leung YK, Ho SM. Androgenic regulation of oxidative stress in the rat prostate: involvement of NAD(P)H oxidases and antioxidant defense machinery during prostatic involution and regrowth. Am J Pathol 2003;163:2513–22.
31. Qin S, Chock PB. Implication of phosphatidylinositol 3-kinase membrane recruitment in hydrogen peroxide-induced activation of PI3K and Akt. Biochemistry 2003;42:2995–3003.
32. Wu F, Peacock SO, Rao S, Lemmon SK, Burnstein KL. Novel interaction between the co-chaperone Cdc37 and Rho GTPase exchange factor Vav3 promotes androgen receptor activity and prostate cancer growth. J Biol Chem 2013;288:5463–74.
33. Li H, Wang Y, Liu X. Plk1-dependent phosphorylation regulates functions of DNA topoisomerase IIalpha in cell cycle progression. J Biol Chem 2008;283:6209–21.
34. Liu XS, Li H, Song B, Liu X. Polo-like kinase 1 phosphorylation of G_2 and S-phase-expressed 1 protein is essential for p53 inactivation during G_2 checkpoint recovery. EMBO Rep 2010;11:626–32.
35. Yang X, Li H, Zhou Z, Wang WH, Deng A, Andrisani O, et al. Plk1-mediated phosphorylation of Topors regulates p53 stability. J Biol Chem 2009;284:18588–92.
36. Li H, Liu XS, Yang X, Wang Y, Turner JR, Liu X. Phosphorylation of CLIP-170 by Plk1 and CK2 promotes timely formation of kinetochore-microtubule attachments. Embo J 2010;29:2953–65.
37. Li H, Liu XS, Yang X, Song B, Wang Y, Liu X. Polo-like kinase 1 phosphorylation of p150Glued facilitates nuclear envelope breakdown during prophase. Proc Natl Acad Sci U S A 2010;107: 14633–8.
38. Hou X, Li Z, Huang W, Li J, Staiger C, Kuang S, et al. Plk1-dependent microtubule dynamics promotes androgen receptor signaling in prostate cancer. Prostate 2013;73:1352–63.
39. Song B, Liu XS, Rice SJ, Kuang S, Elzey BD, Konieczny SF, et al. Plk1 phosphorylation of orc2 and hbo1 contributes to gemcitabine resistance in pancreatic cancer. Mol Cancer Ther 2013;12:58–68.
40. Song B, Liu XS, Davis K, Liu X. Plk1 phosphorylation of Orc2 promotes DNA replication under conditions of stress. Mol Cell Biol 2011;31: 4844–56.
41. Wu ZQ, Liu X. Role for Plk1 phosphorylation of Hbo1 in regulation of replication licensing. Proc Natl Acad Sci U S A 2008;105: 1919–24.
42. Li Z, Li J, Bi P, Lu Y, Burcham G, Elzey BD, et al. Plk1 phosphorylation of PTEN causes a tumor-promoting metabolic state. Mol Cell Biol 2014;34:3642–61.
43. Wilton JH, Titus MA, Efstathiou E, Fetterly GJ, Mohler JL. Androgenic biomarker prof | ling in human matrices and cell culture samples using high throughput, electrospray tandem mass spectrometry. Prostate 2014;74:722–31.